INTERNATIONAL JOURNAL FOR NUMERICAL METHODS IN ENGINEERING
Int. J. Numer. Meth. Engng 2012; **00**:1–25
Published online in Wiley InterScience (www.interscience.wiley.com). DOI: 10.1002/nme

A comparison of techniques for overcoming non-uniqueness of boundary integral equations for the collocation partition of unity method in two dimensional acoustic scattering

G.C. Diwan*†, J. Trevelyan and G. Coates

School of Engineering and Computing Sciences, Durham University, South Road, Durham, DH1 3LE, England.

SUMMARY

The Partition of Unity Method has become an attractive approach for extending the allowable frequency range for wave simulations beyond that available using piecewise polynomial elements. The non-uniqueness of solution obtained from the Conventional Boundary Integral Equation (CBIE) is well known. The CBIE derived through Green's identities suffers from a problem of non-uniqueness at certain characteristic frequencies. Two of the standard methods of overcoming this problem are the so-called CHIEF method and that of Burton and Miller. The latter method introduces a hypersingular integral which may be treated in various ways. In this paper we present the collocation Partition of Unity Boundary Element Method (PUBEM) for the Helmholtz problem and compare the performance of CHIEF against a Burton-Miller formulation regularised using the approach of Li and Huang. Copyright © 2012 John Wiley & Sons, Ltd.

Received . . .

KEY WORDS: Partition of Unity Method, non-uniqueness, CHIEF, Burton-Miller formulation

1. INTRODUCTION

1.1. Partition of Unity Method:

The fundamental work on the Partition of Unity Method (PUM) was carried out by Melenk and Babuška [1] as a generalised Finite Element (FE) technique [2]. The fundamental idea was to use the analytical information of the problem that is being analysed in the FE basis functions. After Melenk and Babuška's work [3] on Helmholtz and elasticity problems, the PUM has further been extended both for FE and BE techniques by Bettess and his co-workers for solving wave problems [4],[5],[6] and by Ortiz and Sanchez for diffraction problems [7]. Farhat et al [8],[9] presented a variant of PUM by using a discontinuous enrichment method. In their work the finite element basis was enriched by adding the plane waves to the polynomial basis instead of multiplication with it. Use

†Email: g.c.diwan@durham.ac.uk
*Correspondence to: School of Engineering and Computing Sciences, Durham University, South Road, Durham, DH1 3LE, England.

of PUM for efficiently solving practical problems in acoustics [10],[11],[12] and in solid mechanics [13] using collocation BEM is also well established. The use of the plane wave enrichment has also been found to be advantageous in Galerkin BEM [14]. The improvement in the accuracy of the numerical solution either by FE or BE techniques and the gain in the efficiency of solving the system equations is widely reported, see [15],[16],[17],[18].

Indeed, the idea of using a priori knowledge of the solution in the approximation space can be attributed to Trefftz. Trefftz's concept was to use the particular solutions in the variational approach for solving the governing partial differential equations [19]. Although introduced in 1926, probably the first generalisation of Trefftz methods for solving practical problem (plate bending) with FEM is due to Jirousek [20] in 1977. Trefftz methods have received a considerable attention in the last two decades in regards to extending their applicability for solving wave problems using either FEM or the Galerkin method. The literature on the techniques based on the Trefftz methods is vast and only a few of the relevant works are mentioned here. More related Trefftz's type works in the wave problems are the Ultra Weak Variational Formulation (UVWF)[21],[22], the Variational Theory of Complex Rays (VTCR) for vibration problems [23], Fourier expansion based VTCR [24], discontinuous Galerkin FEM [25] (Helmholtz equation) and recently [26] (Maxwell equation). Another very recent contribution to UWVF for Helmholtz equation using the first kind Bessel function along with the usual plane waves is due to Luostari et al [27]. Use of plane wave basis also finds its application in transient acoustic [28] and electromagnetic [29] wave scattering problems. The 'Plane Wave Time Domain' (PWTD) algorithm [28],[29] has been shown to cost $\mathcal{O}(N_t N_s^{1.5} \log N_s)$ as aginst conventional BEM that requires $\mathcal{O}(N_t N_s^2)$ operations. Here N_t and N_s are the number of temporal and spatial basis functions needed to approximate the total field. Nair and Shanker use a 'Generalized Method of Moments' (GMM) for solving the integral equation for electromagnetic [30] and acoustic [31] scattering problems. Their algorithm is shown to be flexible in the use of various orders and kinds of basis functions. The condition number of the linear system resulting from their method is shown to be stable over a wide range of frequencies.

As will be discussed in Sec. 3.2, one of the problems in using the plane wave enrichment is the oscillatory behaviour of the plane wave basis. Since the BEM uses fundamental solution in the integral equations (which in turn is wavenumber dependent for acoustic problems), one has to be very careful in evaluating these oscillatory integrals particularly at high frequencies. The algorithm developed by Bruno et al [32] is specifically aimed at handling the oscillatory integrals encountered when solving electromagnetic and acoustic scattering from large, convex obstacles with BEM. Authors in that paper present a formulation and an integration scheme based on the method of stationary phase that enables i) the use of a fixed set of discretization points independent of frequency and ii) the use of the GMRES solver which converges within a fixed number of iterations independent of frequency of the problem. Impressive savings in CPU time are reported. Another algorithm is due to Griebel and Schweitzer [33] for mesh free Galerkin FEM with partition of unity. These authors demonstrate an exponential convergence for the p version of GFEM with the use of a sparse grid integration scheme on non-overlapping cells dividing the integration domain. Bettess et al [4] present a semi-analytical quadrature method for the oscillatory integrals in PUFEM. This however can not straight forward be implemented in PUBEM because of the presence of Green's function in the boundary integrals. Honnor et al [10] use asymptotic expression for the Green's function in 2D followed by a non-oscillatory representation of the integrand in the complex plane

DOI: 10.1002/nme

to perform the quadrature. Although significant savings can be achieved in terms of number of integration points, the method is not entirely robust.

1.2. The non-uniqueness problem

It is well known that the Conventional Boundary Integral Equation (CBIE) for an exterior acoustic problem results in a non-unique solution at irregular frequencies for the corresponding interior problem and that this is a purely mathematical phenomenon. Two of the available approaches to overcome the non-uniqueness are the Combined Helmholtz Integral Equation Formulation (CHIEF) method and the Burton-Miller method. The CHIEF method due to Schenck [34] uses some additional Helmholtz integral equations evaluated at points interior to the scatterer (and exterior to the acoustic domain) which are added in the original system matrix. Although this results in an over-determined system, CHIEF ensures a unique solution at an irregular frequency. These interior points need to be chosen such that they do not lie on the nodal lines of the eigenmodes of the interior Helmholtz problem. This however can introduce uncertainties at high wavenumbers as the nodal lines become densely packed in the interior which makes it difficult to find suitable locations for the placement of interior points. Apart from stating the problem with the interior collocation points when they lie on the nodal lines of the interior modes, Schenck has not provided any criteria as to what number of CHIEF points be chosen to ensure a unique solution. To this effect, some work has been done by Wu and Seybert [35], Juhl [36] to further enhance the CHIEF method to obtain a unique solution. Wu and Seybert propose a weighted residual form of the CHIEF method which can ensure a unique solution using the concept of 'CHIEF block'. A CHIEF block is a volume considered inside the scatterer where the CHIEF equation (or the interior Helmholtz problem) is solved in a weighted residual sense. Juhl's approach on the other hand uses the Singular Value Decomposition (SVD) technique to identify the rank deficiency of the coefficient matrix and with this assess the quality of the CHIEF points. A very important observation of Juhl is about the accuracy with which the scatterer geometry is modelled and the associated possibility to circumvent the non-uniqueness. It is known that the CBIE can result in a non-unique solution at wavenumbers near the eigenvalues of the interior problem for a coarse mesh. This 'band' of spurious wavenumbers is the major concern when solving exterior acoustic problems as one is less likely to solve exactly at a spurious wavenumber. As observed by Juhl, the non-uniqueness in this particular spurious 'band' may be avoided if one uses a very fine mesh. This of course comes at the cost of excessive computation. As will be discussed later, one of the motivations for using Partition of Unity methods (apart from obtaining a very high accuracy), is to be able to use a coarse mesh. It is therefore very crucial that the geometric modelling of the scatterer be accurate for exterior acoustic problems in view of the problem with non-uniqueness in the spurious band. A rigorous analytical and numerical investigation of the CHIEF method has been presented by Chen et al [37] for the spurious eigensolution in a multiply connected domain. There are several other variations of the CHIEF method but their mention is avoided only for brevity. However, for a good discussion on the non-uniqueness problem and on the several enhancements of the CHIEF method, the reader is referred to a review presented by Marburg and Wu (Chapter 15 in [38]).

Another method to avoid the non-uniqueness problem is due to Burton and Miller [39]. They showed that the integral equation resulting from linear combination of the CBIE and its normal

DOI: 10.1002/nme

derivative at the collocation point always results in a unique solution. The major problem with this method is the evaluation of a hypersingular integral which arises as a result of the differentiation of the CBIE at the collocation point. There are various techniques available to handle the hypersingular integral in the Burton-Miller formulation. One such technique is the 'regularisation' procedure which is simply a subtraction of singularity technique (SST) combined with identities from potential theory [40]. Various methods of regularisation for use with the BEM technique for acoustic and elastic scattering problems can be found in [41],[42],[43],[44],[45]. Another technique is due to Guiggiani [46] which is based again on the subtraction of singularity but it does not use the identities from the potential theory. Rather, the technique is based on expanding the singular kernel in a Taylor series using polynomial shape functions. Although mathematically elegant and widely applied for practical problems [47],[13] (Dual BEM for fracture mechanics), [48](Stokes flow in duct), it can become difficult to obtain complicated expansions for the fundamental solutions (the Green's functions). Often an exact geometry is essential in the PUBEM technique [16] (also recall the discussion in Sec. 1.2) and Guiggiani's method can become highly involved when performing the analytical integration on the exact boundary. Also, since the PUBEM is specifically aimed at solving short wavelength problems, the use of an approximate modelling of the scatterer geometry can introduce numerical dispersion in the solution. It is for this reason that we use the regularisation procedure [40] where the singularity subtraction is analytical.

The BEM system of equations, formed using either the CHIEF or Burton-Miller formulation, is dense and often ill-conditioned (in the case of plane wave based methods). This may be become a problem for high frequency problems when using conventional direct solvers as the cost of solving the system scales with $\mathcal{O}(N^3)$ where N is the total number of equations in the BEM system. One of the many techniques to accelerate the BEM solution is the Fast Multipole Method (FMM). An adaptive version of FMM [49],[50] has been used to solve several 3D acoustic scattering problems using Burton and Miller formulation. The authors show that significant savings in CPU time can be achieved compared to the conventional BEM or non-adaptive FMM. Load balancing is known to be a problem for parallel implementation of FMM. Hariharan et al [51] present an algorithm that avoids the load balancing steps and demonstrate considerable speed-up for the parallel FMM for electromagnetic scattering problems.

In this paper we present a comparison between the CHIEF method and the Burton-Miller method for the PUBEM solution of the classical single and multiple exterior acoustic scattering problems in two dimensions. For handling the hypersingular integral in the Burton-Miller formulation, we use the regularisation proposed by Li and Huang [40]. It may be noted that the Burton-Miller formulation contains only weakly singular integrals after the application of the regularisation procedure of Li and Huang to the hypersingular and the strongly singular kernel. The two methods are compared for their accuracy, solution efficiency and conditioning of the coefficient matrix.

DOI: 10.1002/nme

2. GOVERNING EQUATION

The well known equation for time harmonic acoustic scattering and wave propagation is the Helmholtz equation

$$\nabla^2\phi(q) + k^2\phi(q) = 0 \qquad q \in \Omega \tag{1}$$

where k is the acoustic wavenumber, ϕ the spatially dependent ($e^{-i\omega t}$ time dependence) total acoustic potential that we seek in the computational domain Ω and ∇^2 is the Laplacian operator. For exterior acoustic problems, the total (or scattered) acoustic potential has to satisfy Sommerfeld's radiation condition given by

$$\lim_{r\to\infty} r^{\frac{n-1}{2}}\left(\frac{\partial}{\partial r} - ik\right)\phi = 0 \tag{2}$$

where r is the distance of a point in Ω from the origin, n is the dimension of the space and $i = \sqrt{-1}$. The mathematical formulation for deriving the CBIE from the Helmholtz equation is well established [52]. The CBIE for an acoustic scattering (or radiation) problem governed by the Helmholtz differential equation is given by

$$c(p)\phi(p) + \int_\Gamma \frac{\partial G}{\partial n_q}\phi(q)d\Gamma(q) = \int_\Gamma G\frac{\partial\phi(q)}{\partial n_q}d\Gamma(q) + \phi^i(p), \quad p, q \in \Gamma \tag{3}$$

where p is the collocation or source point, q the field point, G the free space Green's function for the Helmholtz problem, n_q the outward normal at point q on the boundary Γ, $\phi(q)$ the unknown acoustic potential and $\phi^i(p)$ the known incident acoustic wave. The term $c(p)$ is the free coefficient which depends on the local geometry of Γ at p. In this study we assume Γ is smooth and take $c(p) = \frac{1}{2}$. Thus when the normal derivative of the acoustic potential is prescribed on the boundary, (3) can be used to compute the acoustic potential.

The Green's function for the Helmholtz equation in two-dimensions is given by

$$G = \frac{i}{4}H_0(kr) \tag{4}$$

where $H_0(\cdot)$ is the first kind Hankel function of order zero. The normal derivative of (3) at the collocation point p is given by

$$c(p)\frac{\partial\phi(p)}{\partial n_p} + \int_\Gamma \frac{\partial^2 G}{\partial n_p \partial n_q}\phi(q)d\Gamma(q) = \int_\Gamma \frac{\partial G}{\partial n_p}\frac{\partial\phi(q)}{\partial n_q}d\Gamma(q) + \frac{\partial\phi^i(p)}{\partial n_p} \tag{5}$$

and the Combined Hypersingular BIE (CHBIE) due to Burton and Miller [39] is

$$\begin{aligned} &c(p)\phi(p) + \alpha c(p)\frac{\partial\phi(p)}{\partial n_p} + \int_\Gamma \frac{\partial G}{\partial n_q}\phi(q)d\Gamma(q) + \alpha\int_\Gamma \frac{\partial^2 G}{\partial n_p\partial n_q}\phi(q)d\Gamma(q) = \\ &\int_\Gamma G\frac{\partial\phi(q)}{\partial n_q}d\Gamma(q) + \alpha\int_\Gamma \frac{\partial G}{\partial n_p}\frac{\partial\phi(q)}{\partial n_q}d\Gamma(q) + \phi^i(p) + \alpha\frac{\partial\phi^i(p)}{\partial n_p} \end{aligned} \tag{6}$$

where α is a coupling constant most commonly taken as i/k. In the present study, we analyse the acoustic scattering from sound hard surface(s) for which the normal derivative of the total acoustic potential vanishes. Therefore, all the terms in (6) involving the normal derivative of acoustic potential vanish. Although (6) results in a unique solution, its main drawback remains the numerical

DOI: 10.1002/nme

treatment of the hypersingular integral, i.e. the last integral on the left hand side. Li and Huang [40] presented the following weakly singular form of the hypersingular integral

$$\int_\Gamma \frac{\partial^2 G}{\partial n_p \partial n_q}\phi(q)d\Gamma(q) = \int_\Gamma \left[\frac{\partial^2 G}{\partial n_p \partial n_q} - \frac{\partial^2 G_0}{\partial n_p \partial n_q}\right]\phi(q)\Gamma(q) \tag{7}$$
$$+ \int_\Gamma \left[\phi(q) - \phi(p) - \nabla\phi(p)\cdot(q-p)\right]\frac{\partial^2 G_0}{\partial n_p \partial n_q}d\Gamma(q)$$
$$+ \int_\Gamma \nabla\phi(p)\cdot n_q \frac{\partial G_0}{\partial n_p}d\Gamma(q) - \frac{1}{2}\nabla\phi(p)\cdot n_p$$

where G_0 is the free space Green's function for the Laplace equation and is given as

$$G_0 = \frac{1}{2\pi}\ln\left(\frac{1}{r}\right). \tag{8}$$

Again, for the present case of a hard boundary, the last term in the right hand side of (7) vanishes. Consequently, the final equation for this case of a hard boundary can be expanded as

$$c(p)\phi(p) + \int_\Gamma \frac{\partial G}{\partial n_q}\phi(q)d\Gamma(q) + \alpha\int_\Gamma \left[\frac{\partial^2 G}{\partial n_p \partial n_q} - \frac{\partial^2 G_0}{\partial n_p \partial n_q}\right]\phi(q)\Gamma(q) \tag{9}$$
$$+ \alpha\int_\Gamma \left[\phi(q) - \phi(p) - \nabla\phi(p)\cdot(q-p)\right]\frac{\partial^2 G_0}{\partial n_p \partial n_q}d\Gamma(q) +$$
$$\alpha\int_\Gamma \nabla\phi(p)\cdot n_q \frac{\partial G_0}{\partial n_p}d\Gamma(q) = \phi^i(p) + \alpha\frac{\partial \phi^i(p)}{\partial n_p}.$$

3. PLANE WAVE BASIS AND AND DISCRETIZATION OF CHBIE

We now introduce the plane wave basis for approximation of the acoustic potential at a point $\mathbf{x}$ on the boundary Γ

$$\phi(\mathbf{x}) = \sum_{j=1}^{J} N_j \sum_{m}^{M_j} A_{jm} e^{ik\mathbf{d}_{jm}\cdot\mathbf{x}} \qquad \mathbf{x}\in\Gamma, \tag{10}$$

where N_j is the j^{th} shape function, A_{jm} the unknown which can be thought of as the amplitude of the m^{th} plane wave with wave number k associated with node j. The direction of the m^{th} plane wave at node j is given by the unit vector $\mathbf{d}_{jm}$ and $\mathbf{x}$ is the location of point where the potential ϕ is sought. (10) is general in the sense that the total number of nodes J on an element and the associated total number of waves with each node, M_j, can vary on the boundary Γ. In the context of the BEM, the plane wave basis defined in (10) can be used to express the unknown acoustic potential on the boundary Γ. There are significant changes introduced when moving from the conventional polynomial basis to plane wave basis viz.

- the unknowns are now the amplitudes of the plane waves (A_{jm}) located around boundary element nodes as against the nodal potential in case of polynomial basis,
- with the use of the plane wave basis, it is possible to use much larger elements for modelling the boundary Γ. A typical boundary element with plane wave approximation can

DOI: 10.1002/nme

accommodate many wavelengths as against the use of a minimum ten nodes per wavelength with the polynomial basis, and,

- the exponential function in the plane wave basis makes the associated integrals highly oscillatory in nature. This necessitates special attention when performing the numerical integration.

It is now convenient to write the following discretized form of (9) using (10)

$$C_1 + \sum_{s=1}^{s=4} \sum_{e=1}^{n_e} I_s^e = C_2 + C_3 \tag{11}$$

where

$$C_1 = c(p) \sum_{j=1}^{3} N_j^p \sum_{m=1}^{M_j} A_{jm}^p e^{ik\mathbf{d}_{jm}\cdot\mathbf{x}(p)} \tag{12}$$

$$I_1^e = \int_{\Gamma^e} \left(\frac{\partial G}{\partial n_q} \right) \sum_{j=1}^{3} N_j^q \sum_{m=1}^{M_j} A_{jm}^q e^{ik\mathbf{d}_{jm}\cdot\mathbf{x}(q)} d\Gamma^e(q) \tag{13}$$

$$I_2^e = \alpha \int_{\Gamma^e} \frac{\partial^2 G}{\partial n_q \partial n_p} \left(\sum_{j=1}^{3} N_j^q \sum_{m=1}^{M_j} A_{jm}^q e^{ik\mathbf{d}_{jm}\cdot\mathbf{x}(q)} - \sum_{j=1}^{3} N_j^p \sum_{m=1}^{M_j} A_{jm}^p e^{ik\mathbf{d}_{jm}\cdot\mathbf{x}(p)} \right) d\Gamma^e(q) \tag{14}$$

$$I_3^e = \alpha \int_{\Gamma^e} \frac{\partial^2 G_0}{\partial n_p \partial n_q} \left(\left(\sum_{j=1}^{3} N_j^q \sum_{m=1}^{M_j} A_{jm}^q e^{ik\mathbf{d}_{jm}\cdot\mathbf{x}(q)} - \sum_{j=1}^{3} N_j^p \sum_{m=1}^{M_j} A_{jm}^p e^{ik\mathbf{d}_{jm}\cdot\mathbf{x}(p)} \right) - \left(\frac{\partial}{\partial x} \left[\sum_{j=1}^{3} N_j^p \sum_{m=1}^{M_j} A_{jm}^p e^{ik\mathbf{d}_{jm}\cdot\mathbf{x}(p)} \right] r_x + \frac{\partial}{\partial y} \left[\sum_{j=1}^{3} N_j^p \sum_{m=1}^{M_j} A_{jm}^p e^{ik\mathbf{d}_{jm}\cdot\mathbf{x}(p)} \right] r_y \right) d\Gamma^e(q) \tag{15}$$

$$I_4^e = \alpha \int_{\Gamma^e} \left(\frac{\partial}{\partial x} \left[\sum_{j=1}^{3} N_j^p \sum_{m=1}^{M_j} A_{jm}^p e^{ik\mathbf{d}_{jm}\cdot\mathbf{x}(p)} \right] n_{qx} + \frac{\partial}{\partial y} \left[\sum_{j=1}^{3} N_j^p \sum_{m=1}^{M_j} A_{jm}^p e^{ik\mathbf{d}_{jm}\cdot\mathbf{x}(p)} \right] n_{qy} \right) d\Gamma^e(q) \tag{16}$$

and

$$C_2 = \phi^i(p) \;\; ; \;\; C_3 = \alpha \frac{\partial \phi^i(p)}{\partial n_p} \tag{17}$$

where n_e is the total number of boundary elements dividing the boundary Γ and Γ^e is the division of Γ corresponding to the e^{th} boundary element, A_{jm}^p (A_{jm}^q) the amplitude of m^{th} plane wave associated with j^{th} node on the element that contains the collocation point p (field point q), N_j^p (N_j^q) the polynomial shape function for node j of the element containing the collocation point p (field point q), n_{qx} and n_{qy} the x and y components of the unit outward normal at point q on the boundary Γ. $r_x = x(q) - x(p)$ and $r_y = y(q) - y(p)$ where x and y are simply the Cartesian coordinates. Choosing appropriate locations on the boundary Γ as collocation points p yields the

DOI: 10.1002/nme

following set of linear equations

$$[\mathbf{H}]\{\mathbf{a}\} = \{\mathbf{b}\} \tag{18}$$

where the vector $\mathbf{a}$ contains the amplitudes of plane waves. Vector $\mathbf{b}$ is obtained as

$$\{\mathbf{b}\} = \{\mathbf{C_2} + \mathbf{C_3}\} \tag{19}$$

where $\{\mathbf{C_2}\}$ and $\{\mathbf{C_3}\}$ are the vectors formed using (17). The matrix $\mathbf{H}$ is obtained by evaluating the boundary integrals. The solution of linear system (18) yields the amplitudes of the plane waves, A_{jm} which can be used to quickly recover the acoustic potential on the boundary Γ using (10).

3.1. Collocation

As mentioned earlier, the PUBEM necessitates the use of an exact geometry to obtain accurate results. We therefore use the exact geometry of the scatterer so that Γ^e becomes analytical and is given as

$$\Gamma^e = \{\gamma^e(\xi) : -1 \leq \xi \leq 1\}. \tag{20}$$

It is a common practice in the conventional BEM to use the boundary element nodes as the collocation points. However, in view of (10), we require additional collocation points as the total number of unknowns has now increased to $2 \times n_e \times M$ as against $2 \times n_e$ for conventional collocation BEM, for the case of a 3-noded continuous element. It is therefore convenient to write,

$$p_s = \left\{ \gamma^e(\xi) : \xi = a - 2 + \frac{m-1}{M} \right\} \; a = 1, 2, \; m = 1, 2, ..M. \tag{21}$$

where $s = 1, 2, ..., 2M$, $2M$ being the total number of degrees of freedom for the element Γ^e. It follows immediately that (21) generates the collocation points p_s that are regularly spaced in $\{\xi : -1 \leq \xi \leq 1\}$. A theoretical restriction on the continuity of the acoustic potential requires further attention to the placement of point p in the case where two adjacent elements are concerned. A frequently mentioned problem with the continuous elements for the use with hypersingular integrals is the Hölder continuity requirement on the density function (or the acoustic potential in the present case). The Hölder continuity requirement needs the density functions to be $C^{1,\alpha}$ continuous whereas the continuous elements are only $C^{0,\alpha}$ continuous at the inter-element edges. Although satisfactory results have been presented by violating this condition [41], we will follow a collocation strategy where the collocation points always lie entirely inside an element which automatically satisfies the $C^{1,\alpha}$ condition [53].

3.2. Numerical integration

It is known that the boundary integrals in (9) become oscillatory in nature due to the introduction of the plane wave basis apart from the inherent oscillatory nature of the fundamental solution present in the kernel of the integral equation, i.e., the Green's function. A complicating factor for the integration is that the PUBEM formulation encourages the use of elements spanning many wavelengths, so there is the requirement to evaluate accurately highly oscillatory integrals. Apart from the requirement of using an analytical geometry where possible, accuracy of the PUBEM solution heavily depends on how accurately these oscillatory integrals are evaluated. We use a

DOI: 10.1002/nme

subdivision of the $-1 \leq \xi \leq 1$ interval into C cells of equal size to evaluate the oscillatory integrals using Gauss quadrature. In the present work, we use 10 Gauss points per cell, and cells of length approximately equal to $\lambda/3$. We acknowledge the more sophisticated integration schemes cited in Sec. 1.1, but adopt this scheme, namely, element subdivision in C equal length cells, for its robustness. To make this concept clear, let us rewrite one of the boundary integrals, say I_1^e (see (13)),

$$I_1^e = \int_{\Gamma^e} \left(\frac{\partial G}{\partial n_q} \right) \sum_{j=1}^{3} N_j^q \sum_{m=1}^{M_j} A_{jm}^q e^{ik\mathbf{d}_{jm}\cdot\mathbf{x}(q)} d\Gamma^e(q) \tag{22}$$

Using the first parametric mapping (20), I_1^e can be written as

$$I_1^e = \int_{\xi=-1}^{\xi=1} \left(\frac{\partial G}{\partial n_q} \right) \sum_{j=1}^{3} N_j^q \sum_{m=1}^{M_j} A_{jm}^q e^{ik\mathbf{d}_{jm}\cdot\mathbf{x}(q)} J(\xi) d\xi(q) \tag{23}$$

where $J(\xi)$ is the Jacobian of transformation $\Gamma^e \rightarrow \xi$. Now, using the division of the ξ interval in C cells, we can write (23) as

$$I_1^e = \sum^{C} \int_{\eta=-1}^{\eta=1} \left(\frac{\partial G}{\partial n_q} \right) \sum_{j=1}^{3} N_j^q \sum_{m=1}^{M_j} A_{jm}^q e^{ik\mathbf{d}_{jm}\cdot\mathbf{x}(q)} J(\eta) d\eta(q). \tag{24}$$

Now η is the local coordinate in each individual cell and $J(\eta)$ is the Jacobian of transformation $\Gamma^e \rightarrow \eta$. It should be noted that even after the regularisation, the integrals in (9) that contain derivatives of the Green's function are still weakly singular. This requires a suitable coordinate transformation to be applied so that the integrals are evaluated correctly. Out of the several coordinate transformation methods available, we compare the performance of four different methods for evaluating the weakly singular integrals in (9). The coordinate transformations methods investigated here are i) Telles [54], ii) Monegato - Sloan (MS [55]), iii) bicubic [56] and iv) Wu's transformation [57]. The Telles and MS transformations are applied in the entire local interval $\eta \in (-1, 1)$ if it contains the singular point, p. Bicubic and Wu's scheme, on the other hand, split this local interval (η) towards the left and right of the singularity (p) and then apply the transformation in each individual interval. In the next section we present error analyses for two acoustic scattering problems namely i) scattering from a single sound hard cylinder and ii) scattering from an array of four cylinders. This will be followed by an example of acoustic scattering from a long sound hard capsule to examine the stability of the CHIEF method alone.

4. SCATTERING FROM SOUND HARD CYLINDER(S)

Before we present the error analyses for the cylinder problems, it will be prudent to define a parameter τ which gives the number of degrees of freedom per wavelength for a given problem, i.e.,

$$\tau = \frac{T}{ka} \tag{25}$$

DOI: 10.1002/nme

where T is the total number of degrees of freedom in the system for one cylinder and a is the radius of the cylinder. Thus for the problem of scattering from a single cylinder with unit radius, $\tau = T/k$ where T will be simply the multiplication of the total number of nodes on the scatterer boundary and number of plane waves per node. It should be noted that we use one integration cell per collocation point and thus the total number of degrees of freedom T (in 25) is equal to the total number of integration cells used on the boundary of one cylinder, i.e,

$$T = n_e \times C \tag{26}$$

Note that C is the number of integration cells per element (see 24). For all the results presented here the parameter $\tau \approx 3.0$ unless otherwise mentioned. This value has been found to be sufficient to recover solutions with acceptable engineering accuracy of 1% and moderate condition numbers which can be effciently handled with the SVD algorithm, see [16]. For smooth scatterers this accuracy will be shown to be much better ($\approx 10^{-4}$). Also all the results are obtained with 30 integration (Gauss) points per wavelength unless otherwise mentioned. For both the single cylinder and four cylinder examples, we use two 3-noded continuous elements per cylinder along with the trigonometric shape functions presented by Peake et al [12]. Thus the single cylinder case has only two continuous elements and the four cylinder case uses 8 continuous elements. For all computations the integration points are placed analytically on the scatterer boundary. We now define the relative L^2 error for the total acoustic potential ϕ on the boundary Γ, $E^2(\phi)$ as

$$E^2(\phi) = \frac{\|\phi - \tilde{\phi}\|}{\|\tilde{\phi}\|} \tag{27}$$

where ϕ is the numerically computed solution and $\tilde{\phi}$ the analytical solution computed using the infinite or approximate series for a given scattering problem. The coefficient matrix $\mathbf{H}$ generated using the plane wave basis is always highly ill-conditioned. A typical condition number for the coefficient matrix $\mathbf{H}$ for a moderately high value of $k > 100$ is $\approx 10^{15}$. The problem of poorly conditioned systems because of the use of the plane waves has been widely reported, see the discussion in [17] and the references therein. In general, the condition number for a plane wave enriched BEM grows as the wavenumber increases. Clearly, in order to obtain accurate and reliable results from such highly ill-conditioned systems one must ensure that sufficient arithmetic precision is maintained in the computation of the matrix terms. We use double precision arithmetic for all the computations in this study. A natural choice for obtaining accurate solution from the ill-conditioned system (18) is therefore the SVD technique. The applicability of SVD for obtaining accurate solutions from ill-conditioned systems is very well established and the readers may be referred to the benchmark paper by Golub and Kahan [58] for the underlying theory. In this paper, we obtain the solution vector $\mathbf{a}$ in (18) by solving the following complex linear least squares problem:

$$\min \|\mathbf{b} - \mathbf{H}\mathbf{a}\|^2 \tag{28}$$

using the SVD of $\mathbf{H}$.

DOI: 10.1002/nme

The 2-norm condition number for the matrix $\mathbf{H}$, $\kappa(\mathbf{H})$ may be defined as

$$\kappa(\mathbf{H}) = \frac{\sigma_{\max}(\mathbf{H})}{\sigma_{\min}(\mathbf{H})} \tag{29}$$

where $\sigma_{\max}(\mathbf{H})$ and $\sigma_{\min}(\mathbf{H})$ are respectively the maximum and minimum singular values of the matrix $\mathbf{H}$ computed using the SVD. Relevant routines from the LAPACK library are used to solve (28) [59]. As discussed in Sec. 1.2, the placement of interior collocation points for the CHIEF method can become an issue. For the numerical examples presented in this paper, the interior points are placed completely randomly in the interior of the cylinder(s). The number of interior points (or the number of CHIEF equations) used here is 20% of the total number of equations in (18) since this has been found to give stable results for the CHIEF method. Also the CHIEF points in the interior of the cylinder(s) are placed such that they are sufficiently away from the boundary.

4.1. Scattering from a single sound hard cylinder

We first investigate the performance of CHIEF and Burton-Miller methods for the classical problem of plane wave scattering from an acoustically hard cylinder of infinite extent. The analytical solution for the scattered potential on the surface of a hard cylinder centred at origin $(0, 0)$ due to an incident acoustic plane wave with direction $(-1, 0)$ is given by the infinite series [60].

$$\phi^s(\mathbf{x}) = -\frac{\mathrm{J}_0'(ka)}{\mathrm{H}_0'(ka)}\mathrm{H}_0(kr) - 2\sum_{\nu=1}^{\infty} i^{\nu}\frac{\mathrm{J}_\nu'(ka)}{\mathrm{H}_\nu'(ka)}\mathrm{H}_\nu(kr)\cos(\nu\theta), \tag{30}$$

where $\mathbf{x} = r(\cos(\theta), \sin(\theta))$, $\mathrm{H}_\nu(\cdot)$ is the Hankel function of the first kind and order ν, $\mathrm{J}_\nu(\cdot)$ is the Bessel function of the first kind and order ν. The prime sign denotes a derivative with respect to kr. The total acoustic potential ϕ can be computed by simply performing a complex addition of incident wave to the scattered potential given by (30), i.e., $\phi = \phi^i + \phi^s$. The relative L^2 error for the total acoustic potential is then computed using (27).

4.1.1. Truncated SVD

Before proceeding to the error analyses for the scattering problems with different coordinate transformation schemes for singular integrals, we first present results that demonstrate the ability of SVD to produce stable and accurate results via the single cylinder scattering problem. As mentioned earlier, the coefficient matrix $\mathbf{H}$ is ill-conditioned (or rank deficient) and this makes the problem stated in (28) ill-posed because a small perturbation in the right hand side vector $\mathbf{b}$ can result in a significantly large perturbation in the solution vector $\mathbf{a}$. It is therefore important to be able to solve (28) reliably when $\kappa(\mathbf{H})$ is significantly high to obtain stable and accurate solution. In the present study, we use the truncated SVD routine ZGELSS from LAPACK to solve (28). The idea used in ZGELSS is to obtain a minimum $||a||$ solution from the set of least squares solutions that minimize $\|\mathbf{b} - \mathbf{H}\mathbf{a}\|^2$ over a solution space that is spanned by the singular vectors with singular values greater than ϵ_0, where ϵ_0 is the user input for the truncation threshold of singular values. This essentially means filtering out those singular values from the SVD of $\mathbf{H}$ that are below ϵ_0 and solve (28) with a modified $\mathbf{H}$, possibly with an improved rank. A well known method to estimate

DOI: 10.1002/nme

the suitable value for the parameter ϵ_0 is the so called L-curve method [61]. Fig. 1 shows the L-curves for (18) for the problem of plane wave scattering from a single cylinder for three different wavenumbers, namely, $k = 32$, $k = 100$ and $k = 150$. The singular values (σ_c) computed using SVD for each wavenumber case corresponding to the respective L-curve corner points are also shown in Fig. 1. For eg. the corner value for $k = 32$ is $\sigma_c(k = 32) = 1.82\text{E-}04$, indicating that it is possible to obtain accurate solution by truncating the singular values that are below $\sigma_c(k = 32)$, i.e. by setting ϵ_0 = 1.82E-04 for $k = 32$ case. Although the threshold value ϵ_0 is dependent on the wavenumber of the problem being solved, in this paper, we take the threshold ϵ_0 = 1.0E-10, as this was found to give satisfactory results for all the examples considered. This is demonstrated through numerical results for various values of ϵ_0 as shown in Fig. 2. The results shown in Fig. 2 are only for the CHIEF method, however, similar behaviour is observed in the results for the Burton-Miller method as well. As seen from Fig. 2, it is clear that the SVD algorithm with ϵ_0 = 1.0E-10 produces stable results with very good accuracy.

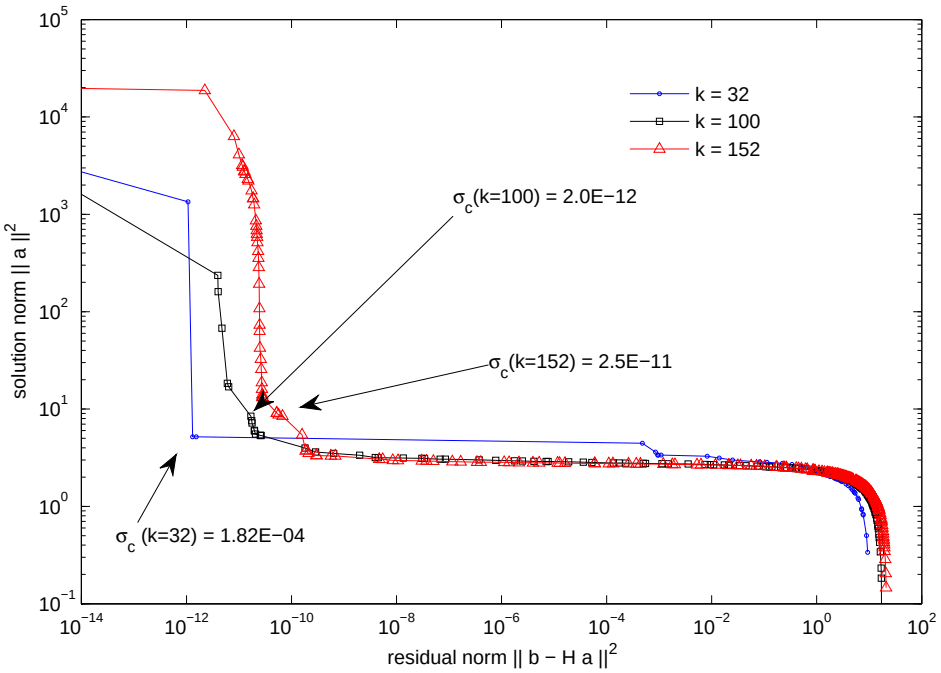

Figure 1. L-curve for (28) for scattering from single cylinder.

4.1.2. Comparison of CHIEF and Burton-Miller methods with singular integration schemes

We now present the comparison between the CHIEF and the Burton-Miller methods with various singular integration schemes. Fig. 3 shows the relative L^2 error, $E^2(\phi)$ for CHIEF and Burton-Miller methods and Fig. 4 gives the comparison for the condition number defined in (29). The multiple lines for the Burton-Miller method in Figs. 3-4 correspond to various coordinate transformation schemes used to handle the weakly singular integrals.

DOI: 10.1002/nme

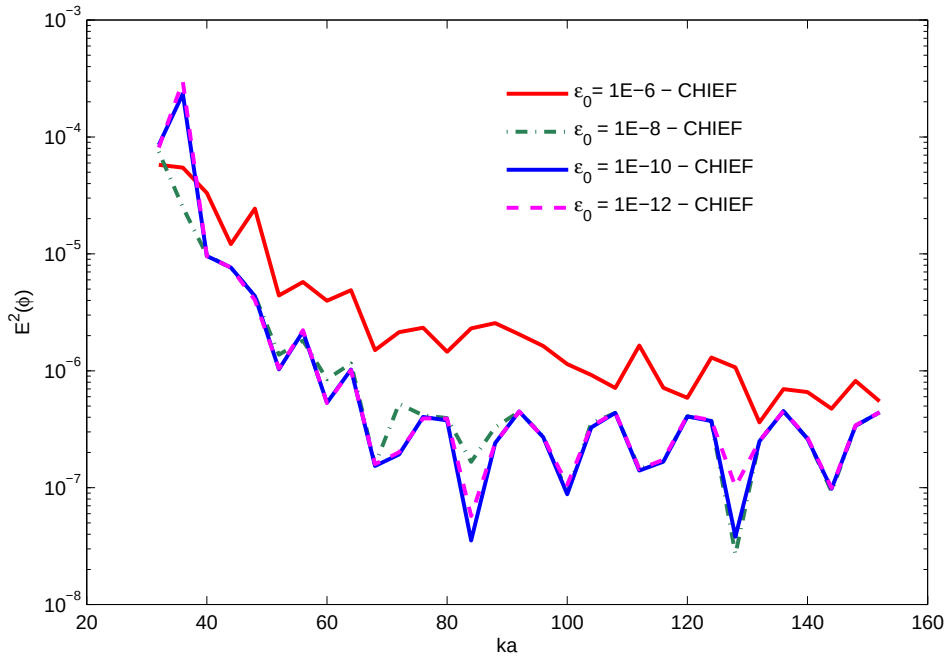

Figure 2. PUBEM results for various values of ϵ_0 for single cylinder problem.

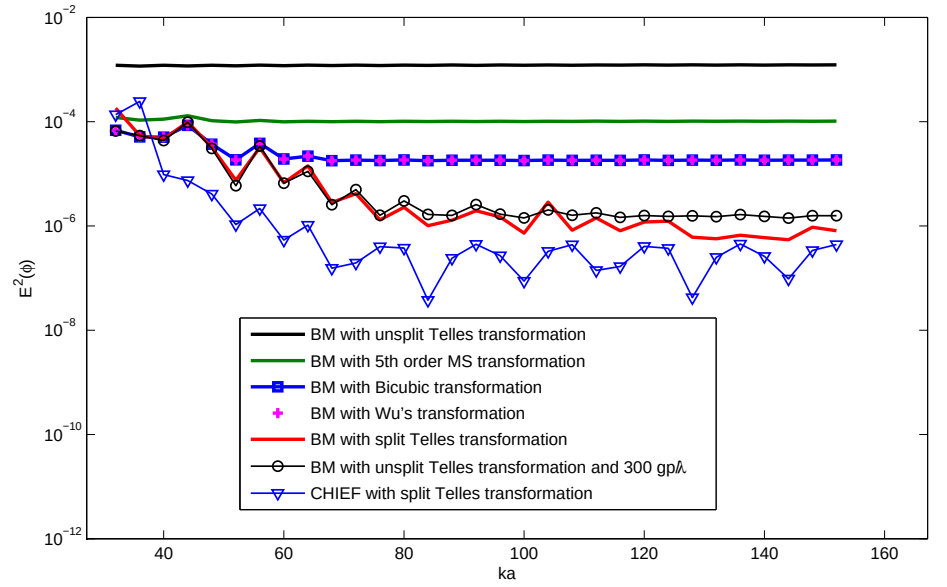

Figure 3. $E^2(\phi)$ for the single cylinder problem.

As seen from Fig.3, CHIEF provides better accuracy compared to Burton-Miller results obtained with various singular integration schemes mentioned earlier at 30 integration points per wavelength. Note that when the weak singularity in (9) is handled with the Telles scheme without splitting the interval containing the singularity ($\eta \in (-1, 1)$), the Burton-Miller formulation needs at least

DOI: 10.1002/nme

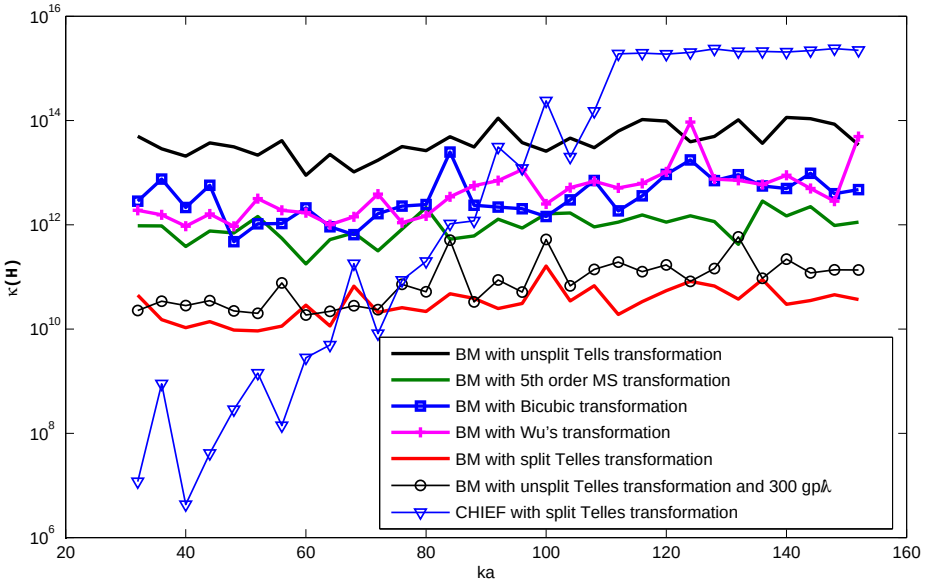

Figure 4. $\kappa(\mathbf{H})$ for the single cylinder problem.

300 integration points per wavelength to achieve a comparable accuracy to that of CHIEF with 30 integration points per wavelength. It should be mentioned here that although the regularised form of the Burton-Miller formulation used here is only weakly singular, the third integral on the left hand side of (9) converges extremely slowly. Consequently, Burton-Miller needs a very high number of integration points in order to achieve an accuracy comparable to that from the CHIEF method, if it uses the Telles transformation without interval splitting. The efficacy of the Telles scheme for handling the weakly singular integrals has been investigated by many researchers,[56],[62],[63]. It is clear from these studies that the Telles transformation when used without partitioning gives poor results. Singh and Tanaka[62] report at least 3 orders of magnitude improvement for a logarithmic singularity when the Telles transformation is used with the partition of the interval for 10 Gauss points. We see from Fig.3 that splitting the local interval $\eta \in (-1, 1)$ indeed improves the Burton-Miller result in comparison with the result obtained without splitting the interval. Similar numerical experiments carried out with conventional polynomial BEM show that the L_2 errors with various singular integration schemes discussed do not vary significantly. For instance, the L_2 errors for the single cylinder problem using the quadratic discontinuous elements are of the $\mathcal{O}(10^{-3})$ for all the singular integration schemes discussed and for $\tau = 20$. The collocation points used are the nodal locations of the discontinuous element which is a common practice followed in conventional polynomial BEM. We use discontinuous elements for polynomial BEM in order to satisfy the Hölder continuity requirement on the hypersingular integral. It is found that when the element nodes are used as the collocation points, the convergence of the slowly converging integral in (9) mentioned earlier is possible with relatively low number (10 to 12) of Gauss points irrespective of the singular integration scheme used. Therefore, the results obtained with various singular integration schemes remain within the same order of magnitude for polynomial BEM. This disparity in the results with various singular integration schemes for PUBEM and polynomial BEM can be attributed to the fact

DOI: 10.1002/nme

that the collocation points used in PUBEM are not element nodes causing the integrals for PUBEM to converge slowly.

The condition numbers for CHIEF for $k < 64$ are better in comparison with Burton-Miller but degrade with increasing k (see Fig.4). Interestingly an accurately computed Burton-Miller solution provides a better conditioning of the system matrix. Amini and Harris [64] studied the dependence of the condition number on the wavenumber k. The numerical examples they presented are with conventional BEM and with $k < 20$ for a 3D problem. It follows from their work that the condition number for a regularised Burton-Miller formulation increases steadily with growing k and the coupling parameter α. In a PUBEM context, as shown in Fig. 4, the ill-conditioning arising from the plane wave basis is the dominant effect and the steady increase noticed by Amini and Harris is no longer evident. However, despite the very high condition numbers encountered, the SVD algorithm is able to find a unique solution. It is evident from Fig. 3 that the PUBEM implementations of both CHIEF and Burton-Miller are accurate and stable over the range of wavenumbers considered here.

As mentioned before, the number of CHIEF equations used for the CHIEF results shown in Fig. 3 is 20% of the total equations in the system (18) and that their locations in the interior are completely random. This randomness can practically guarantee that there will always be enough CHIEF points to provide the linear independence needed to obtain a unique solution.

4.2. Scattering from an array of four cylinders

The scattering from a multi-cylinder array presents a more challenging case as it involves multiple reflections from individual cylinders which ultimately forms the total acoustic field. The recursive multiple reflections make this problem an ideal candidate to test the efficacy of PUBEM to obtain an accurate solution. We consider a setting of four unit radius sound hard cylinders of infinite extent with their centres placed at (-2,-2), (2,-2), (2,2) and (-2,2) in a two dimensional homogeneous unbounded acoustic medium (air). A unit amplitude plane wave with wavenumber k is taken to be incident on this cylinder array at an angle of $\theta^I = 45^\circ$ with the horizontal. There are various methods to solve a multiple scattering boundary value problem such as this and a good review of these methods can be found in [65]. We use the formula proposed by Linton and Evans [66] (eq. 2.15) to compare our PUBEM solution for the total acoustic potential on the surface of each cylinder. The formula proposed by Linton and Evans is based on the addition theorem that combines the separable solutions of Helmholtz equation, see [65] for details. The addition theorems can be efficiently used to compute the solution but the infinite series has to be truncated in practice. Theoretically of course, an infinite sum should result in a converged solution. However, when solving even the truncated system of linear equations, the addition of extra terms in the series can make the system matrix highly ill-conditioned. Fig.5 shows the dependence of the condition number of the system matrix formed from (2.15) in [66] on the number of terms included in the series. Note that $k = 2.4048$ is an irregular wavenumber (first zero of the first kind Bessel function, J_0). Clearly the reason for such significantly high condition numbers is the wide spread of eigenvalues with the growing number of terms in the series.

In light of the result shown in Fig.5 it becomes imperative to find the number of terms needed to include in the series in order to obtain a correct solution from the truncated series. This is because the relative L^2 errors will depend heavily on how accurately the series in [66] is computed. A good discussion on the upper and lower bounds on the number of terms to be included in the series can be

DOI: 10.1002/nme

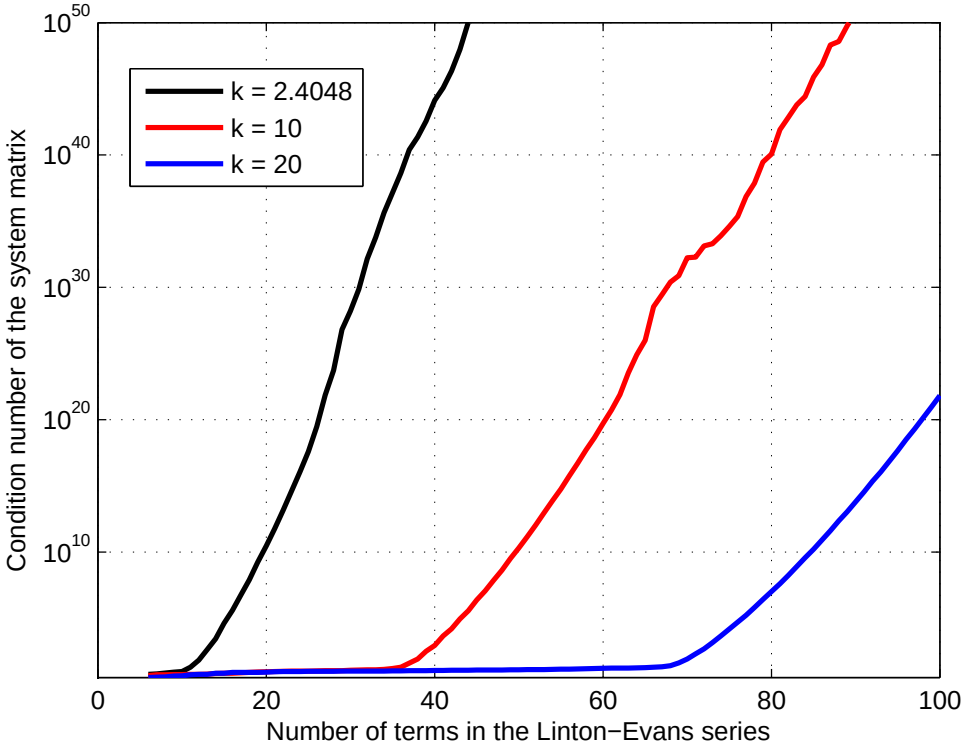

Figure 5. Stability of Linton-Evans series, eq. (2.15) in [66].

found in [67]. More related works from the acoustics domain [68], [69] give an empirical relation for a two cylinder problem, for the number of terms that need to be included for a given value of ka, a being the radius of the cylinder. Recently, Antoine et al [70] have presented an empirical relationship for the number of terms to be used in the infinite series for scattering from multiple circular cylinders

$$M_u = \left[ka_u + \left(\frac{1}{2\sqrt{2}} \ln \left(2\sqrt{2}\pi k a_u \epsilon^{-1} \right) \right)^{\frac{2}{3}} (ka_u)^{\frac{1}{3}} + 1 \right], \tag{31}$$

where M_u is the minimum number of terms that need to be included in the infinite series for u^{th} cylinder with the radius a_u, and ϵ is the desired error bound on the Fourier coefficients that need to be computed in the infinite series. The value of error bound on the Fourier coefficients used by Antonie et al was 10^{-8}. For our case of scattering from identical circular cylinders (all cylinders are unit radius), the number of terms M_u obtained from (31) for each cylinder is the same (say M). We use (31) only as a guideline to find the number of terms (M) needed in the Linton-Evans series (2.15 in [66]) with $\epsilon = 10^{-8}$ in (31). A system of linear equations of size $N_c(2M+1)$ is then formed where N_c is the number of cylinders (4 in the present case). We use a linear least squares solver with QR factorisation to solve this system of linear equations using suitable routines from the LAPACK library and obtain the total acoustic potential on each cylinder surface. This solution is considered as the reference solution and used to compute the relative L^2 error (see (27)) for our PUBEM solution

Prepared using nmeauth.cls
DOI: 10.1002/nme

	Cyl. 1		Cyl. 2		Cyl. 3		Cyl. 4	
	CHIEF	BM	CHIEF	BM	CHIEF	BM	CHIEF	BM
$\tau \approx 3.0$	5.98E-04	1.03	2.15E-04	2.71	2.78E-04	6.26	1.67E-04	2.01
$\tau \approx 3.5$	8.67E-06	4.06E-05	1.28E-05	9.39E-05	7.6E-06	3.29E-05	516E-06	3.82E-05
$\tau \approx 3.9$	2.01E-07	4.07E-06	1.87E-07	4.01E-06	3.46E-07	6.32E-06	1.92E-07	5.17E-06

Table I. PUBEM results - $E^2(\phi)$ for scattering from four cylinder array for $k = 36.9171$ and $\theta^I = 45^\circ$, 100 terms in Linton-Evans series.

	Cyl. 1		Cyl. 2		Cyl. 3		Cyl. 4	
	CHIEF	BM	CHIEF	BM	CHIEF	BM	CHIEF	BM
$\tau \approx 2.2$	43.80	39.34	24.83	16.80	30.95	20.84	24.52	28.28
$\tau \approx 2.6$	7.66E-05	2.30E-03	1.27E-04	4.72E-03	3.52E-04	3.10E-02	8.88E-05	5.17E-03
$\tau \approx 3.0$	3.77E-07	8.18E-06	5.65E-07	1.09E-05	5.08E-07	9.83E-06	5.78E-07	2.04E-05

Table II. PUBEM results - $E^2(\phi)$ for scattering from four cylinder array for $k = 100$ and $\theta^I = 45^\circ$, 150 terms in Linton-Evans series.

	Cyl. 1		Cyl. 2		Cyl. 3		Cyl. 4	
	CHIEF	BM	CHIEF	BM	CHIEF	BM	CHIEF	BM
$\tau \approx 2.2$	8.26	15.26	12.53	27.67	42.43	98.36	15.68	37.90
$\tau \approx 2.6$	6.73E-05	3.0E-03	7.30E-05	2.6E-03	7.23E-05	4.8E-03	7.98E-05	7.0E-03
$\tau \approx 3.0$	6.48E-05	6.47E-05	6.40E-05	6.39E-05	6.68E-05	6.70E-05	6.40E-05	6.46E-05

Table III. PUBEM results - $E^2(\phi)$ for scattering from four cylinder array for $k = 150$ and $\theta^I = 45^\circ$, 200 terms in Linton-Evans series.

k = 36.9171		
	CHIEF	BM
$\tau \approx 3.0$	3.78E+08	1.01E+10
$\tau \approx 3.5$	3.67E+09	1.39E+10
$\tau \approx 3.9$	1.31E+12	1.24E+11

Table IV. PUBEM conditioning - $\kappa(\mathbf{H})$ for CHIEF and regularised Burton-Miller method for four cylinder problem, $k = 36.9171$.

with the CHIEF and Burton-Miller methods. For the error analysis of the four cylinder problem, we consider three cases of the wavenumber, namely, $k = 36.9171$, k = 100 and k = 150. It may be noted that out of the three cases mentioned, $k = 36.9171$ and $k = 150$ are irregular wavenumbers. The regularised Burton-Miller results included for comparison here are obtained with the Telles scheme for the weakly singular integrals in conjunction with splitting the interval $\eta \in (-1, 1)$. The L^2 error results shown in Tables I-III are obtained using two continuous elements per cylinder with trigonometric shape functions as before. All the results are obtained with 30 integration points per wavelength. The condition numbers for the first case of $k = 36.9171$ is given in Table IV and for the latter two cases of $k = 100, 150$ in Table V.

We have used $M = 100$ for $k = 36.9171$, M =150 for $k = 100$, and M =200 for $k = 150$, in the Linton-Evans series. It may be noted that the number of terms used for the cases studied here (M)

DOI: 10.1002/nme

	$k = 100$		$k = 150$	
	CHIEF	BM	CHIEF	BM
$\tau \approx 2.2$	1.35E+06	6.54E+05	2.88E+07	4.46E+07
$\tau \approx 2.6$	1.32E+08	9.41E+09	2.07E+11	2.13E+10
$\tau \approx 3.0$	3.0E+14	2.89E+10	9.96E+14	5.11E+10

Table V. PUBEM conditioning - $\kappa(\mathbf{H})$ for CHIEF and regularised Burton-Miller method for four cylinder problem.

is higher than those prescribed by (31) and this is done in order to obtain the maximum possible accuracy for the solution obtained from Linton-Evans series. We reiterate the fact that the errors listed in Tables I-III are for the particular number of terms used in the Linton-Evans series. A thorough investigation into the stability issues of the superposition methods is beyond the scope of this paper and the reader may be referred to the textbook of Martin for a complete review [71]. The condition number of the coefficient matrix for the Linton-Evans series for $k = 36.9171$ with 100 terms was 14.28, for $k = 100$ with 150 terms was 12.28 and that for $k = 150$ with 200 terms was 16.29. It can be noted from Tables I-III that the accuracy of both CHIEF and regularised Burton-Miller methods improves with more plane waves per node i.e. by increasing the value of the parameter τ. Finally we present a polar plot for the total acoustic potential, ϕ, on the surface of the first cylinder with centre at (-2,-2) for the case of $k = 150$ (Fig. 6). The case of $k = 150$ is chosen as at such a high wavenumber, the recursive reflections give rise to an interesting scattering pattern. An additional plot is shown in Fig. 7 for the same case but only for the region $\theta \in [0, \frac{\pi}{4}]$ on the first cylinder where θ is measured anticlockwise. This is the region where the effect of recursive reflections is the most prominent. The plots shown correspond to the result presented in Table III with $\tau = 3.0$. From Figs. 6-7 , it is evident that the PUBEM solution is able to capture efficiently a complex pattern of the scattered wave at a reasonably high wavenumber. It is not possible to distinguish the CHIEF and Burton-Miller results from Linton-Evans series solution as all three of them visually lie on top of each other.

5. SCATTERING FROM A LONG CAPSULE

It is known that the density of characteristic wavenumbers for a given scatterer geometry increases as the wavenumber increases. As noted earlier, this is a major concern for the CHIEF method when choosing the interior collocation points. For an elongated object the problem may get worse as the characteristic wavenumbers get very closely spaced. For this purpose, we will investigate PUBEM implementation of only the CHIEF method for an elongated body. In order to study this problem, we consider the geometry that of a long capsule (Fig. 8). The overall length of the capsule is $(b + 2R)$ where b is the length of the straight edge and R is the radius of the semicircular end of the capsule. A few cases are presented for two values of the ratio b/a, where a is the perimeter of the semicircular end. For all the cases, three noded continuous elements with trigonometric shape functions are used. The integration points are placed analytically on the geometry. As before, the value of parameter τ is taken as 3.0. Since we intend to investigate the performance of CHIEF method at high wavenumbers, it will be convenient to define the relative L_2 error in total acoustic potential on the boundary of

DOI: 10.1002/nme

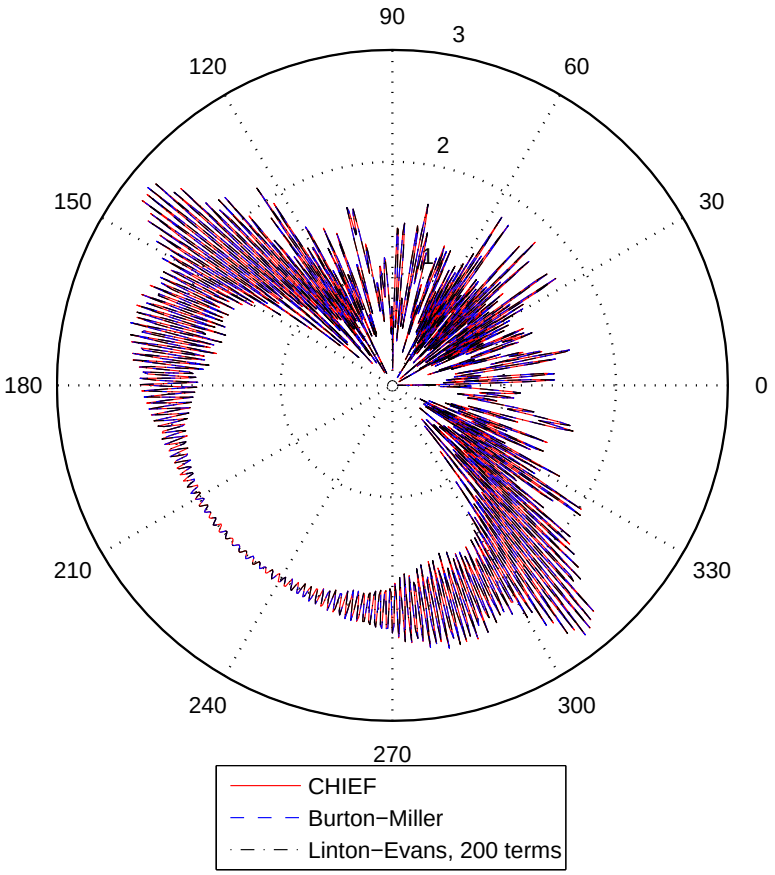

Figure 6. $|\phi|$ for cylinder 1, $k = 150$.

capsule as

$$E^2(\phi_j) = \frac{\|\phi_j - \phi_1\|}{\|\phi_1\|} \tag{32}$$

where ϕ_j is the solution obtained from j^{th} instance of CHIEF method and ϕ_1 is the solution from the first instance of CHIEF method at a given wavenumber. Note that for each instance of the CHIEF method, the location of the interior collocation points will be different as they are positioned completely randomly each time. Therefore solution at every instance from CHIEF method will differ from each other. This potentially forms the basis for testing the stability of the method for elongated geometry where the characteristic wavenumbers are very closely spaced. A total of hundred instances are tried for each case to examine the stability of the CHIEF method. For this problem, each of the semicircular end of the capsule is modelled with one element. The parameters used for this problem are summarized in Table VI.

As is evident from Fig. (9), the CHIEF method is stable even for a considerably elongated geometry at $b/a = 10$ and 20. For such a geometry, one would expect the eigenvalues for the interior Dirichlet problem to be extremely close to each other making CHIEF method susceptible to find the correct solution. However as seen from Fig. (9), the strategy described earlier to position the

DOI: 10.1002/nme

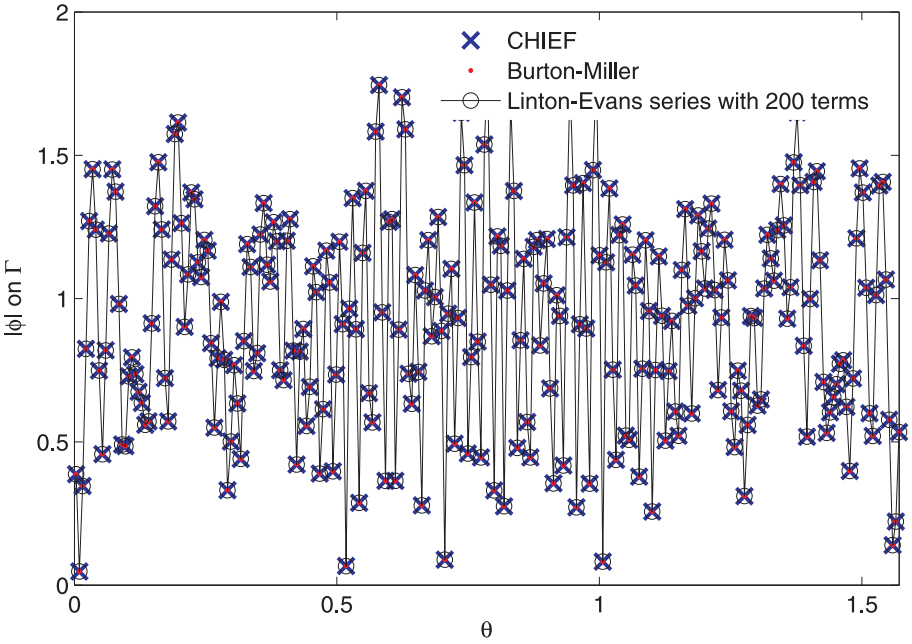

Figure 7. $|\phi|$ for cylinder 1 for $\theta \in [0, \frac{\pi}{4}]$, $k = 150$.

b/a	k	P/λ	n_e	T
10	48	528	22	1548
10	100	1100	22	3300
20	32	672	42	2016
20	64	1344	42	4032

Table VI. Parameters for capsule problem, $P = 2a + 2b$, T: total degrees of freedom for capsule problem.

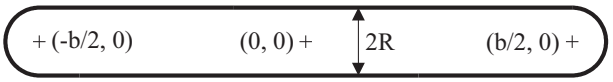

Figure 8. Capsule geometry.

CHIEF points completely randomly with sufficient offset from the boundary gives good results. Interestingly, the CHIEF results become increasingly stable as the wavenumber increases. Note that two of the cases solved here have more than 1000 wavelengths around the scatterer which is a particularly attractive problem to be solved with PUBEM.

6. CONCLUSIONS

1. We have presented a plane wave enriched BEM formulation of the regularised Burton-Miller equations for the exterior acoustic scattering problem in two dimensions. The error analyses presented for the classical single and the multiple scattering problems show that the CHIEF method outperforms Burton-Miller method by at least 1 order of magnitude for the problems

DOI: 10.1002/nme

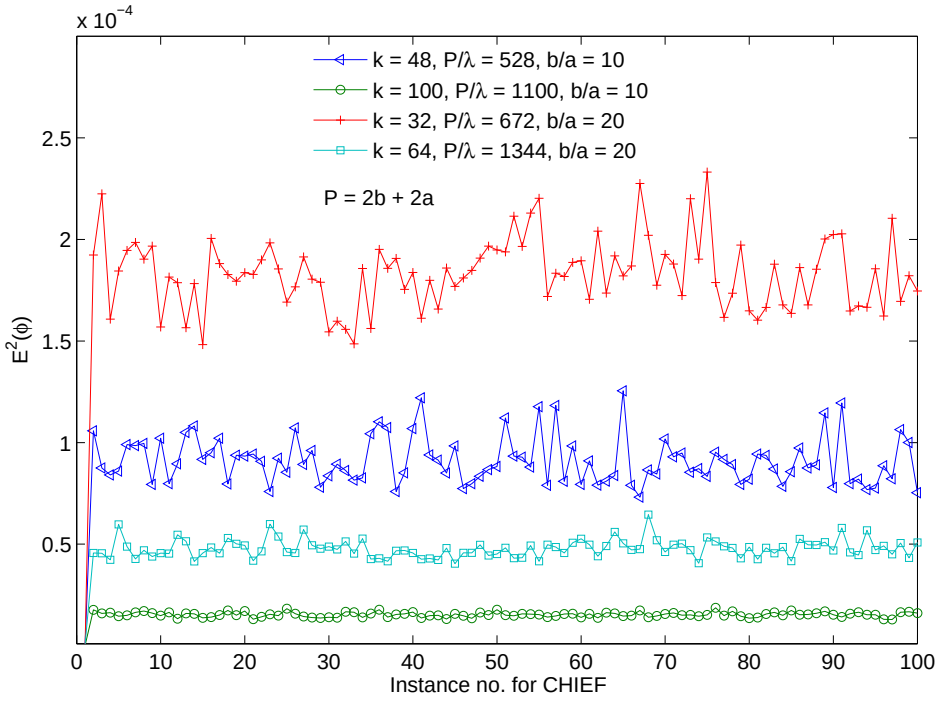

Figure 9. $E^2(\phi)$ for the capsule problem.

considered in this paper. The Burton-Miller method can prove competitive despite the difficult and slowly converging integrals if suitable coordinate transformations are implemented. Investigation of several coordinate transformation techniques for the weakly singular integrals in the regularised Burton-Miller formulation shows that the Telles transformation with interval splitting is the most accurate method. For both single and multiple scattering problems, the enriched form of the regularised Burton-Miller formulation has smaller condition numbers when compared to the CHIEF method. The last example shows that the CHIEF results are stable even for an elongated capsule problem for the medium range of wavenumbers. This indicates that the CHIEF method may be preferred over the Burton-Miller formulation, at least for simpler geometries and moderate wavenumbers ($k < 200$) as the former does not have the problem of hypersingular integrals and provided that a sufficient number of interior collocation points are chosen that ensure the linear independence of the coefficient matrix $\mathbf{H}$. The stability and accuracy of the PUBEM scheme have both been clearly demonstrated in previous works [12],[15],[16],[18] and here we provide further evidence. In Fig.9, we show the stability through repeated instances of the CHIEF formulation, and highly accurate solutions are demonstrated in Figs. 3, 7 and Tables I-III.

2. *Future work*: *Iterative solver:* As demonstrated via results presented in the paper, the number of degrees of freedom per wavelength (τ) needed for PUBEM is close to 3 for the examples considered and can go below 3 for higher wavenumbers. This is 3-4 times smaller than that required in the polynomial based BEM where τ needs to be ≈ 10 to obtain solutions within the engineering accuracy of 1-2%. For 3D cases, the benefits are substantially increased since

DOI: 10.1002/nme

the factor of 3-4 applies in two orthogonal directions [15]. However, this substantial saving in τ comes at the cost of solving the linear system with SVD which costs $\mathcal{O}(N^3)$ operations. In view of the computational cost involved at higher wavenumbers than those considered in this paper, further study and development of iterative solvers with efficient preconditioners is needed.

Scattering from non-smooth obstacles and 3D problems: Wave scattering from sharp tips or from non-smooth obstacles can be modelled with the present PU based algorithm, though, for such problems, Bessel function basis is more suitable, see [72]. Numerical results (not included here) for plane wave scattering from a single cylinder indicate that $\tau \approx 8$ is needed in order to achieve an accuracy $\mathcal{O}(10^{-4})$ when Bessel functions are used in the basis thus indicating the plane wave to be more efficient for the smooth geometries considered here . The results presented are expected to extend to 3D problems, however, for a proper comparison, an appropriate convergence of the integrals in the regularized form of Burton-Miller formulation needs to be ensured. Also, previous study by E. Perrey-Debain et al [15] shows that the conditioning of the coefficient matrix improves for 3D problems making it possible to use more efficient solvers than SVD, such as QR decomposition.

REFERENCES

1. Babuška I, Melenk JM. The partition of unity method. *International Journal for Numerical Methods in Engineering* 1997; **40**(4):727–758.
2. Melenk J, Babuška I. The partition of unity finite element method: basic theory and applications. *Computer Methods in Applied Mechanics and Engineering* 1996; **139**(1):289–314.
3. Melenk J, Babuška I. Approximation with harmonic and generalized harmonic polynomials in the partition of unity method. *Computer Assisted Mechanics and Engineering Sciences* 1997; **4**:607–632.
4. Bettess P, Shirron J, Laghrouche O, Peseux B, Sugimoto R, Trevelyan J. A numerical integration scheme for special finite elements for the Helmholtz equation. *International Journal for Numerical Methods in Engineering* 2003; **56**(4):531–552.
5. Sugimoto R, Bettess P, Trevelyan J. A numerical integration scheme for special quadrilateral finite elements for the Helmholtz equation. *Communications in Numerical Methods in Engineering* 2002; **19**(3):233–245.
6. Laghrouche O, Bettess P, Perrey-Debain E, Trevelyan J. Wave interpolation finite elements for Helmholtz problems with jumps in the wave speed. *Computer Methods in Applied Mechanics and Engineering* 2005; **194**(2):367–381.
7. Ortiz P, Sanchez E. An improved partition of unity finite element model for diffraction problems. *International Journal for Numerical Methods in Engineering* 2001; **50**(12):2727–2740.
8. Farhat C, Harari I, Franca L. The discontinuous enrichment method. *Computer Methods in Applied Mechanics and Engineering* 2001; **190**(48):6455–6479.
9. Farhat C, Harari I, Hetmaniuk U. A discontinuous Galerkin method with lagrange multipliers for the solution of Helmholtz problems in the mid-frequency regime. *Computer Methods in Applied Mechanics and Engineering* 2003; **192**(11):1389–1419.
10. Honnor ME, Trevelyan J, Huybrechs D. Numerical evaluation of the two-dimensional partition of unity boundary integrals for Helmholtz problems. *Journal of Computational and Applied Mathematics* Jul 2010; **234**(6):1656–1662.
11. Arden S, Chandler-Wilde SN, Langdon S. A collocation method for high-frequency scattering by convex polygons. *Journal of Computational and Applied Mathematics* 2007; **204**(2):334–343.
12. Peake M, Trevelyan J, Coates G. Novel basis functions for the partition of unity boundary element method for Helmholtz problems. *International Journal for Numerical Methods in Engineering* 2012; .
13. Simpson R, Trevelyan J. A partition of unity enriched dual boundary element method for accurate computations in fracture mechanics. *Computer Methods in Applied Mechanics and Engineering* 2011; **200**(1):1–10.
14. Chandler-Wilde S, Langdon S. A Galerkin boundary element method for high frequency scattering by convex polygons. *SIAM Journal on Numerical Analysis* 2007; **45**(2):610–640.

DOI: 10.1002/nme

15. Perrey-Debain E, Laghrouche O, Bettess P, Trevelyan J. Plane-wave basis finite elements and boundary elements for three-dimensional wave scattering. *Philosophical Transactions of the Royal Society of London. Series A: Mathematical, Physical and Engineering Sciences* 2004; **362**(1816):561–577.
16. Perrey-Debain E, Trevelyan J, Bettess P. Plane wave interpolation in direct collocation boundary element method for radiation and wave scattering: numerical aspects and applications. *Journal of Sound and Vibration* 2003; **261**(5):839 – 858.
17. Laghrouche O, Bettess P, Astley RJ. Modelling of short wave diffraction problems using approximating systems of plane waves. *International Journal for Numerical Methods in Engineering* 2002; **54**(10):1501–1533.
18. Perrey-Debain E, Trevelyan J, Bettess P. New special wave boundary elements for short wave problems. *Communications in Numerical Methods in Engineering* 2002; **18**(4):259–268.
19. Herrera I. Trefftz method: a general theory. *Numerical Methods for Partial Differential Equations* 2000; **16**(6):561–580.
20. Jirousek J, Leon N. A powerful finite element for plate bending. *Computer Methods in Applied Mechanics and Engineering* 1977; **12**(1):77 – 96.
21. Cessenat O, Despres B. Application of an ultra weak variational formulation of elliptic pdes to the two-dimensional Helmholtz problem. *SIAM J. Numer. Anal*. Feb 1998; **35**(1):255–299.
22. Huttunen T, Monk P, Kaipio J. Computational aspects of the ultra-weak variational formulation. *Journal of Computational Physics* 2002; **182**(1):27–46.
23. Ladeveze P, Arnaud L, Rouch P, Blanzé C. The variational theory of complex rays for the calculation of medium-frequency vibrations. *Engineering Computations* 2001; **18**(1/2):193–214.
24. Kovalevsky L, Ladeveze P, HRiou. The fourier version of the variational theory of complex rays for medium-frequency acoustics. *Computer Methods in Applied Mechanics and Engineering* 2012; **225228**(0):142–153.
25. Gittelson C, Hiptmair R, Perugia I. Plane wave discontinuous Galerkin methods: Analysis of the h-version. *ESAIM: Mathematical Modelling and Numerical Analysis* 2009; **43**(02):297–331.
26. Hiptmair R, Moiola A, Perugia I. Error analysis of Trefftz-discontinuous Galerkin methods for the time-harmonic Maxwell equations. *Mathematics of Computation* 2013; **82**:247–268.
27. Luostari T, Huttunen T, Monk P. The ultra weak variational formulation using Bessel basis functions. *Communications in Computational Physics* 2012; **11**(2):400.
28. Ergin A, Shanker B, Michielssen E. Fast analysis of transient acoustic wave scattering from rigid bodies using the multilevel plane wave time domain algorithm. *The Journal of the Acoustical Society of America* 2000; **107**:1168.
29. Shanker B, Ergin AA, Aygun K, Michielssen E. Analysis of transient electromagnetic scattering from closed surfaces using a combined field integral equation. *Antennas and Propagation, IEEE Transactions on* 2000; **48**(7):1064–1074.
30. Nair NV, Shanker B. Generalized method of moments: A novel discretization technique for integral equations. *Antennas and Propagation, IEEE Transactions on* 2011; **59**(6):2280–2293.
31. Nair N, Shanker B, Kempel L. Generalized method of moments: A boundary integral framework for adaptive analysis of acoustic scattering. *The Journal of the Acoustical Society of America* 2012; **132**:1261.
32. Bruno OP, Geuzaine CA, Monro JA, Reitich F. Prescribed error tolerances within fixed computational times for scattering problems of arbitrarily high frequency: the convex case. *Philosophical Transactions of the Royal Society of London. Series A: Mathematical, Physical and Engineering Sciences* 2004; **362**(1816):629–645.
33. Griebel M, Schweitzer M. A particle-partition of unity method–part ii: Efficient cover construction and reliable integration. *SIAM Journal on Scientific Computing* 2002; **23**(5):1655–1682, doi:10.1137/S1064827501391588. URL http://epubs.siam.org/doi/abs/10.1137/S1064827501391588.
34. Schenck HA. Improved integral formulation for acoustic radiation problems. *Journal of the Acoustical Society of America* 1968; **44**(1):41–58.
35. Wu T, Seybert A. A weighted residual formulation for the CHIEF method in acoustics. *The Journal of the Acoustical Society of America* 1991; **90**:1608.
36. Juhl P. A numerical study of the coefficient matrix of the boundary element method near characteristic frequencies. *Journal of sound and vibration* 1994; **175**(1):39–50.
37. Chen J, Lin J, Kuo S, Chyuan S. Boundary element analysis for the Helmholtz eigenvalue problems with a multiply connected domain. *Proceedings of the Royal Society of London. Series A: Mathematical, Physical and Engineering Sciences* 2001; **457**(2014):2521–2546.
38. Marburg S, Wu T. *Computational acoustics of noise propagation in fluids-Finite and Boundary Element Methods*, chap. 15. Springer, 2008.
39. Burton A, Miller G. The application of integral equation methods to the numerical solution of some exterior boundary-value problems. *Proceedings of the Royal Society of London. Series A, Mathematical and Physical Sciences* 1971; **323**(1553):201–210.

40. Li S, Huang Q. An improved form of the hypersingular boundary integral equation for exterior acoustic problems. *Engineering Analysis with Boundary Elements* 2010; **34**(3):189–195.
41. Liu Y, Rizzo F. A weakly singular form of the hypersingular boundary integral equation applied to 3-D acoustic wave problems. *Computer Methods in Applied Mechanics and Engineering* 1992; **96**(2):271 – 287.
42. Hwang WS. Hypersingular boundary integral equations for exterior acoustic problems. *The Journal of the Acoustical Society of America* 1997; **101**(6):3336–3342.
43. Chien CC, Rajiyah H, Atluri SN. An effective method for solving the hyper-singular integral equations in 3-D acoustics. *The Journal of the Acoustical Society of America* 1990; **88**(2):918–937.
44. Liu Y, Rudolphi T. Some identities for fundamental solutions and their applications to weakly-singular boundary element formulations. *Engineering Analysis with Boundary Elements* 1991; **8**(6):301–311.
45. Li S, Huang Q. A fast multipole boundary element method based on the improved Burton–Miller formulation for three-dimensional acoustic problems. *Engineering Analysis with Boundary Elements* 2011; **35**(5):719–728.
46. Guiggiani M, Krishnasamy G, Rudolphi T, Rizzo F. A general algorithm for the numerical solution of hypersingular boundary integral equations. *ASME Journal of Applied Mechanics* 1992; **59**(3):604–614.
47. Mi Y, Aliabadi M. Dual boundary element method for three-dimensional fracture mechanics analysis. *Engineering Analysis with Boundary Elements* 1992; **10**(2):161 – 171.
48. Silva JR, Power H, Wrobel L. A hypersingular integral equation formulation for Stokes' flow in ducts. *Engineering Analysis with Boundary Elements* 1993; **12**(3):185 – 193.
49. Shen L, Liu Y. An adaptive fast multipole boundary element method for three-dimensional acoustic wave problems based on the burtonmiller formulation. *Computational Mechanics* 2007; **40**(3):461–472.
50. Wu H, Liu Y, Jiang W. A fast multipole boundary element method for 3d multi-domain acoustic scattering problems based on the burton–miller formulation. *Engineering Analysis with Boundary Elements* 2012; **36**(5):779–788.
51. Hariharan B, Aluru S, Shanker B. A scalable parallel fast multipole method for analysis of scattering from perfect electrically conducting surfaces. *Supercomputing, ACM/IEEE 2002 Conference*, 2002; 42–42, doi:10.1109/SC.2002.10012.
52. Ciskowski R, Brebbia C. *Boundary Element Methods in Acoustics*. CMP and Elsevier Applied Science, 1991.
53. Krishnasamy G, Rizzo F, Rudolphi T. Continuity requirements for density functions in the boundary integral equation method. *Computational Mechanics* 1992; **9**(4):267–284.
54. Telles J. A self-adaptive co-ordinate transformation for efficient numerical evaluation of general boundary element integrals. *International Journal for Numerical Methods in Engineering* 1987; **24**(5):959–973.
55. Monegato G, Sloan I. Numerical solution of the generalized airfoil equation for an airfoil with a flap. *SIAM Journal on Numerical Analysis* 1997; **34**(6):2288–2305.
56. Cerrolaza M, Alarcon E. A bi-cubic transformation for the numerical evaluation of the Cauchy principal value integrals in boundary methods. *International Journal for Numerical Methods in Engineering* 1989; **28**(5):987–999.
57. Wu T, Seybert A. *Boundary element acoustics: Fundamentals and computer codes*, vol. 7, chap. 2. WIT press, 2000.
58. Golub G, Kahan W. Calculating the singular values and pseudo-inverse of a matrix. *Journal of the Society for Industrial & Applied Mathematics, Series B: Numerical Analysis* 1965; **2**(2):205–224.
59. Anderson E, Bai Z, Bischof C, Blackford S, Demmel J, Dongarra J, Du Croz J, Greenbaum A, Hammarling S, McKenney A, *et al.*. *LAPACK Users' guide*, vol. 9. Society for Industrial Mathematics, 1987.
60. Bowman J, Senior T, Uslenghi P ((eds.)). *Electromagnetic and Acoustic Scattering by Simple Shapes*. North-Holland Pub. Co., 1970.
61. Hansen PC. The L-Curve and its use in the numerical treatment of inverse problems. *in Computational Inverse Problems in Electrocardiology, ed. P. Johnston, Advances in Computational Bioengineering*, vol. 4, 2000; 119–142. URL http://citeseerx.ist.psu.edu/viewdoc/summary?doi=10.1.1.33.6040.
62. Singh KM, Tanaka M. On non-linear transformations for accurate numerical evaluation of weakly singular boundary integrals. *International Journal for Numerical Methods in Engineering* 2001; **50**(8):2007–2030.
63. Johnston P. Semi-sigmoidal transformations for evaluating weakly singular boundary element integrals. *International Journal for Numerical Methods in Engineering* 2000; **47**(10):1709–1730.
64. Amini S, Harris P. A comparison between various boundary integral formulations of the exterior acoustic problem. *Computer Methods in Applied Mechanics and Engineering* 1990; **84**(1):59–75.
65. Martin PA. Integral-equation methods for multiple-scattering problems I. Acoustics. *The Quarterly Journal of Mechanics and Applied Mathematics* 1985; **38**(1):105–118.
66. Linton C, Evans D. The interaction of waves with arrays of vertical circular cylinders. *Journal of Fluid Mechanics* 1990; **215**:549–569.
67. Pawliuk P, Yedlin M. Truncating cylindrical wave modes in two-dimensional multiple scattering. *Optics Letters* 2010; **35**(23):3997–3999.

DOI: 10.1002/nme

68. Young J, Bertrand J. Multiple scattering by two cylinders. *The Journal of the Acoustical Society of America* 1975; **58**:1190.
69. Decanini Y, Folacci A, Gabrielli P, Rossi J. Algebraic aspects of multiple scattering by two parallel cylinders: Classification and physical interpretation of scattering resonances. *Journal of Sound and Vibration* 1999; **221**(5):785–804.
70. Antoine X, Chniti C, Ramdani K. On the numerical approximation of high-frequency acoustic multiple scattering problems by circular cylinders. *Journal of Computational Physics* 2008; **227**(3):1754–1771.
71. Martin PA. *Multiple Scattering: Interaction of Time-Harmonic Waves with N Obstacles*, *Encyclopedia of Mathematics and its Applications*, vol. 10. Cambridge University Press, 2006.
72. Betcke T. A GSVD formulation of a domain decomposition method for planar eigenvalue problems. *IMA journal of numerical analysis* 2007; **27**(3):451–478.

DOI: 10.1002/nme